EXPERIMENTAL MEASUREMENT ON AIRFOILS WITH TRAILING EDGE WEDGES

Djoko Sardjadi
PT IPTN, The Indonesian Aircraft Industries, Jl.Pajajaran 154 Bandung Indonesia
or
Aerospace Engineering Department of the Institut Teknologi Bandung,
Jl.Ganesha 10 Bandung 40132 Indonesia

Abstract

Some experimental results on airfoils with trailing edge wedges are presented in this paper. Theoretical analysis is given to understand the physical mechanism how trailing edge wedge works. Trailing edge wedge increases the mean camber line in the trailing edge region where the influence to the airfoil circulation is the most effective. The further aft the increase in camber the larger the increase in circulation. Since a wedge introduces a trailing edge thickness, additional in drag can not be avoided particularly in the low-drag region. It is pointed out here that the trailing edge thickness is becoming an additional parameter in airfoil design. It is introduced, in this paper, briefly a design method that allows one to specify the trailing edge gap to obtain realistic solution with a higher circulation.

Introduction

This paper presents some experimental results of the application of wedges, to form divergent trailing edges, in two-and three-dimensional wing in the low speed regime. The application of divergent trailing edges may give more pronounced advantages in transonic regime than in the low speed regime. However the discussion in the present paper will be limited to the low speed regime only. A brief discussion on the theoretical back ground will be presented first to obtain a more insight into two typical questions, those are, how does it work, and how to design an airfoil with a divergent trailing edge.

An existing wing can be modified to have a divergent trailing edge by adding a wedge to its trailing edge lower surface. Experimental results show that such a wedge shifts the c_l-α curve to the left and shift the c_m-α curve downward. It acts as a cambering device. Since a wedge introduces a trailing edge thickness, additional in drag can not be avoided particularly in the low-drag region. The increase in drag must be kept low such that the lift to drag ration remains high.

Basic ideas

Figure 1 shows inviscid pressure distributions of an airfoil with a wedge added to its trailing edge. It shows that the wedge (divergent trailing edge) induces higher circulation, accelerating the flow over the upper surface and decelerating the flow over the lower surface.

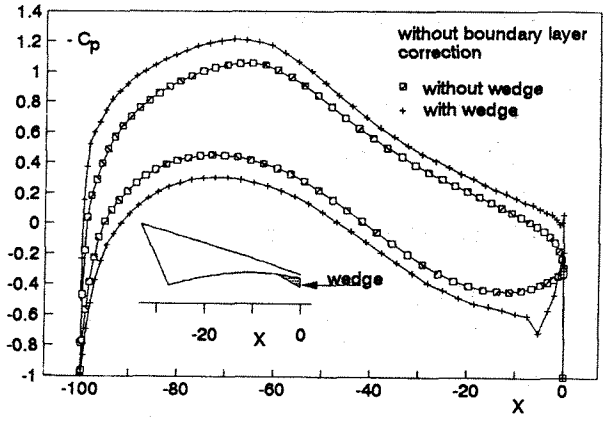

Figure 1. Inviscid pressure distribution of an airfoil with and without a wedge.

It is an evident that a divergent trailing edge induces higher circulation to an airfoil. How does it work? The wedge deflect the airflow downward leaving the airfoil trailing edge. The more the deflection the more the additional in circulation can be obtained. The effectiveness of such a wedge with respect to its relative size can be studied using the classical thin airfoil theory. Consider a flat-plate airfoil with a chord C in an air stream of speed V_0 at zero angle of attack. A hinge point H is introduced to the flat-plate such that the rear part of the airfoil can be deflected to form a plain flap. The flap deflection is indicated by its trailing edge displacement, D. The variations in H and D will be used to express the change in circulation.

From the classical theory we found that the zero lift angle of an airfoil with plain flap is given by

$$\alpha_{L=0} = \frac{1}{\pi}\int_0^{\pi} \frac{dz}{dx}(\cos\theta - 1)d\theta \qquad (1)$$

where $\theta = 0$ and $\theta = \pi$ correspond respectively to the airfoil leading edge and trailing edge, dz / dx is the slope of the airfoil mean camber line. In this study, the flow direction and the airfoil are kept aligned, parallel to the horizontal axis. Hence, dz/dx of the airfoil is zero except for the flap which depends on D and H. Equation (1) can be broken into two parts from $\theta = 0$ to $\theta = \theta_H$ where θ_H is the polar coordinates of the hinge point and from $\theta = \theta_H$ to $\theta = \pi$. The first part results in no contribution since dz/dx is zero. Equation (1) reduces therefore to

$$\alpha_{L=0} = -\frac{1}{\pi}\int_{\theta_H}^{\pi} \frac{dz}{dx}(\cos\theta - 1)d\theta \qquad (2)$$

The slope of the flap is given by

$$\frac{dz}{dx} = \frac{D}{\frac{1}{2}C(1+\cos\theta_H)} \qquad (3)$$

Substituting (3) into (2) results in

$$\alpha_{L=0} = \frac{-2D}{\pi C}\frac{\theta_H - \pi - \sin\theta_H}{\cos\theta_H + 1} \qquad (4)$$

Equation (4) is plotted in figure 2. Figure 2 shows that a smaller plain flap is more effective than the larger one in forming wing camber. As an example, a flap hinged at H = 95% C with a deflection of 0,5% C is as effective as a flap hinged at H = 50%C with a deflection of 5%C. A plain flap hinged at H = 100%C, known as Gurney flap, will be the most effective one.

However, the analysis above was based on an inviscid flow assumption. In a real flow, the following phenomena must obtain sufficient attentions. First, the smaller the plain flap, it may submerged in the boundary layer, hence, the flap becoming less effective. Second, a bubble may present at the corner of the plain flap forming a fixed vortex. The vortex absorbs energy from the outer flow leading to an increase in drag due to the decrease of momentum of the flow leaving the airfoil. Third, a separation may occur on the flap upper surface due to a strong adverse pressure gradient.

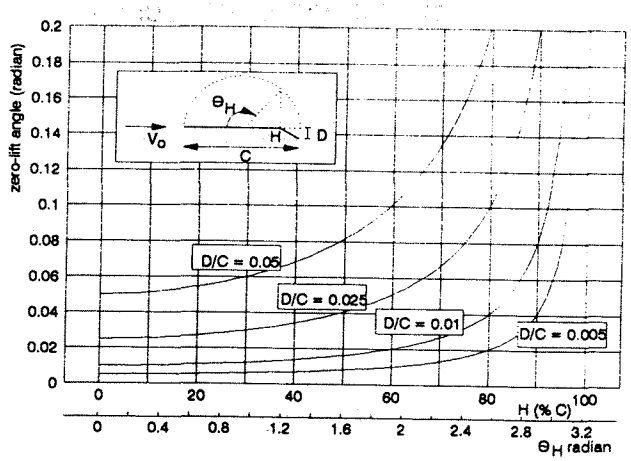

Figure 2. Flat plate airfoil with plain flap.

A wedge

If instead of a plain-flap, a wedge was fixed at the trailing edge lower surface, similar phenomena may still be observed. A trailing edge wedge modifies the mean camber line in the trailing edge region, figure 3.

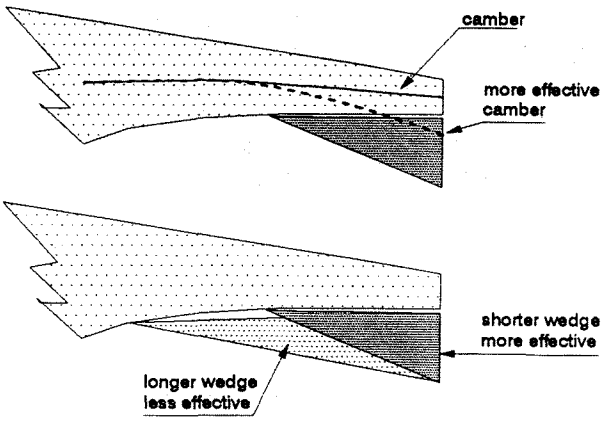

Figure 3. Mean camber line modification by a trailing edge wedge.

Considering the mean camber line to represent the airfoil, hence, for the same trailing edge thickness (wedge thickness) the shorter the wedge the more effective it increases the circulation. It may be expected that a thinner and shorter wedge can be as effective as the thicker and longer one in inducing a certain amount of additional circulation. However, when the wedge size becoming too small it may submerge into the boundary layer which then becoming less effective. A fixed vortex can also be trapped at the corner between the wedge and the airfoil. The shorter the wedge the deeper the corner the stronger the trapped vortex and finally the larger the additional drag. The pressure on the upper

surface can be kept much different from the lower surface pressure distribution up to very close to the trailing edge corners. It is hypothesized that, the key toward this happening, in practice is endorsed by the vortices formation at the trailing edge backward facing surface (base surface). Vortices induce low pressure on the base surface leading to base drag creation. There can be a number of combination of the vortex system down stream the trailing edge base surface to give the same effect for the pressure distribution over the airfoil surface. This hypothesis is used to develop a physical modeling as will be discussed in the subsequent section.

The flow leaving the trailing edge does not violate the Kutta condition in the meaning that the stream trails from the trailing edge upper and lower surfaces smoothly. The flow must not turn around the trailing edge corners but leave the airfoil right at the corners.

Experimental results

Two airfoil were used in the present study. Airfoil # 1 with a maximum thickness of 17% of the chord has a blunt trailing edge, and airfoil # 2 with 18% chord thickness has a sharp trailing edge (figure 4).

wedge nr.	h/c %	l/c %
1	0.5	0.5
2	0.5	1
3	0.5	1.5
4	0.5	2
5	0.25	0.5

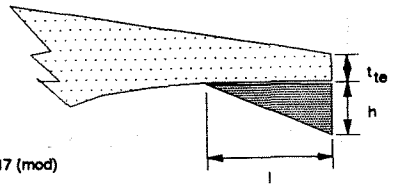

Airfoil # 1 : LS(1)-0417 (mod)

wedge nr.	h/c %	l/c %
1	0.7	2.77
2	0.7	3.37
3	0.7	4.7
4	0.7	7.77
5	0.7	1.57

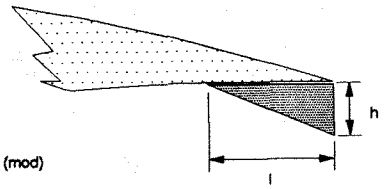

Airfoil # 2 : NACA 65_3-218 (mod)

Figure 4. Airfoils used in the present study.

Figure 4 shows also the wedges used to modify the airfoils trailing edges. Figure 5 shows pressure distributions of the airfoil # 1 with and without the wedges at zero degree angle of attack. This figure confirms the theory described in section 2 that the shorter the wedge, with the same thickness, the larger the increase in circulation. Wedge nr. 5 with a half thickness compared to other wedges, and a half length of wedge nr.1, shows less effect to he pressure distribution compared to wedge nr.1. This wedge is becoming less effective. Figure 6 shows pressure distributions of the airfoil # 2 with and without the wedges. This figures shows also that the shorter wedge influences the pressure distributions more effectively than the longer wedge.

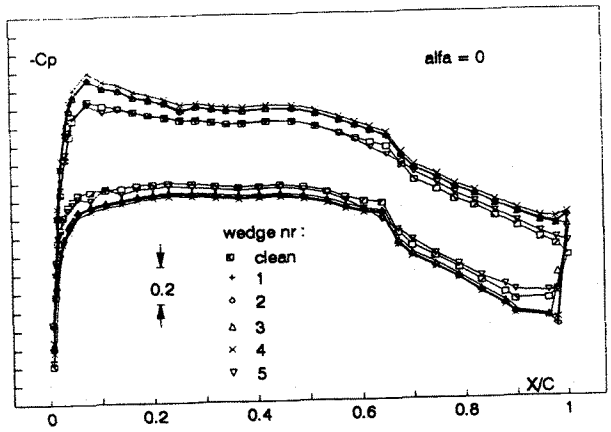

Figure 5. Pressure distribution of the airfoil # 1 with and without the wedges.

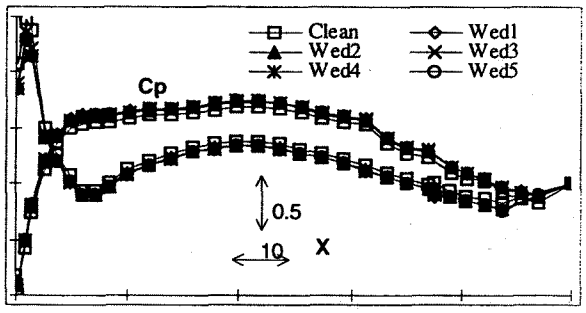

Figure 6. Pressure distribution of the airfoil # 2 with and without the wedges.

Figure 7 and 8, shows the lift, moment, and drag coefficients of the airfoil # 1. The effects of the wedges can be observed clearly in this figure. The maximum increase in lift is given by the wedge nr.4, nevertheless it gives a large increase also in drag as can be seen in figure 8. It seems that the wedge nr.3 gives the best improvement, as can be observed in figure 9, as indicated by the c_l / c_d curves. However at c_l less than 0.6 all the wedges do not improve the airfoil performance. The pitching moment coefficients are becoming more negative due to the increase in circulation.

Figure 10,11, and 12 show the characteristics of the airfoil # 2 with and without wedges. It can be observed also that the shorter the wedge the more effective in increasing the lift but the lager also the accompanying drag increase. Wedge nr.. seems to give the best performance improvement as can be seen in figure 12 as indicated by the c_l / c_d curves.

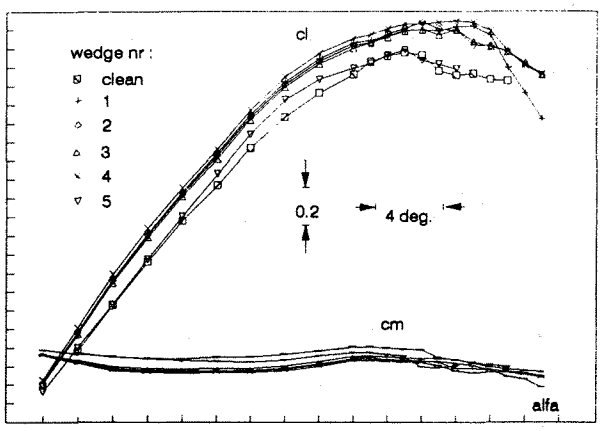

Figure 7. Lift and pitching moment coefficients of the airfoil # 1.

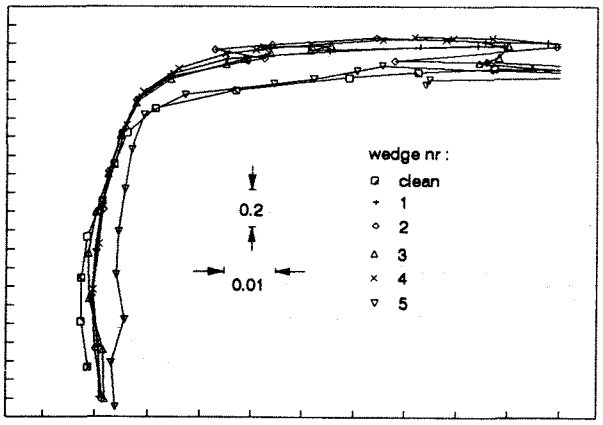

Figure 8. Drag coefficients of the airfoil # 1.

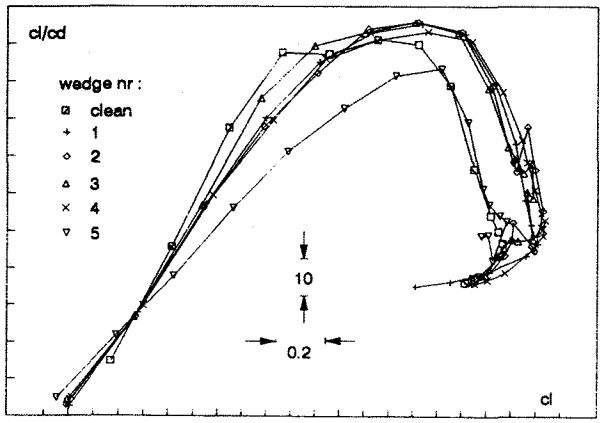

Figure 9. Lift to drag ration of the airfoil # 1.

The experimental results shown above were made in the Nusantara Low Speed Tunnel (NLST) at PT IPTN. The test section is of a rectangular cross section with the dimension of 1100 mm x 1474 mm. The airfoil chord was 400 mm. The measurement were performed at about one million Reynolds number. The c_l, c_d and c_m were computed from the measured pressure distributions on the airfoil surface and the total and static pressures in the wake.

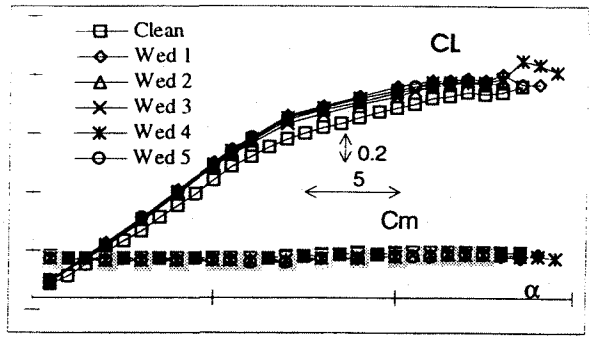

Figure 10. Lift and pitching moment coefficients of the airfoil # 2

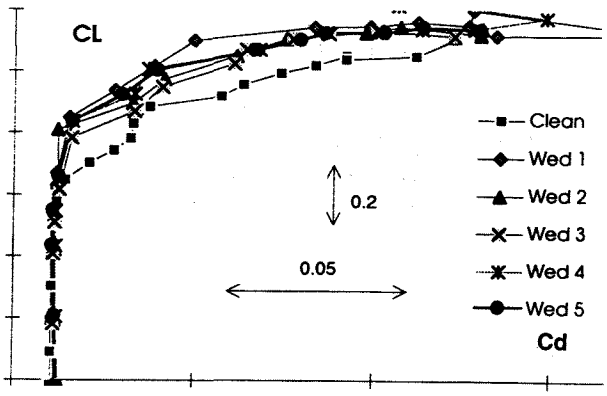

Figure 11. Drag coefficients of the airfoil # 2

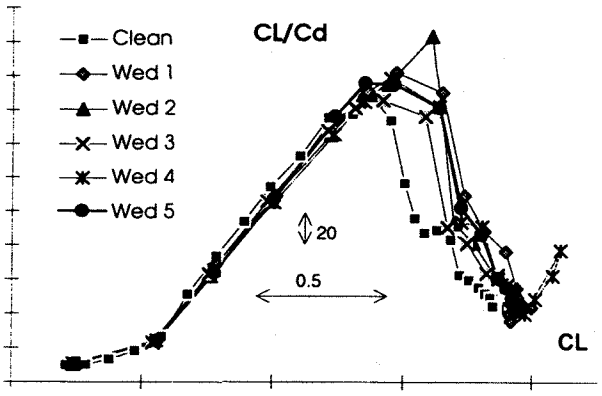

Figure 12. Lift to drag ration of the airfoil # 2

The wedges were attached to the airfoil trailing edge by using double tape and plastered using 0.04 mm tape. A measurement at higher Reynolds number will be conducted mid 1996 in the Indonesian Low Speed Tunnel (ILST) at Serpong. To get better feeling in divergent trailing edge, an experiment using a full span wing with body, of

aspect ratio about 9, was conducted at the ILST. The wing section is of the airfoil # 2 above. The measurement was performed at about one million Reynolds number. The aerodynamic coefficients were derived from the forces measurement using a 6-component external balance. The wedges used in the 3-D measurement were the first three of those used in the 2-D measurement.

Figure 13 and 14 show the lift, moment and drag coefficients of the wing with and without the wedges. The effectiveness of the wedge in increasing the lift still can be found in a finite wing. As in the 2-D cases, an improvement in aerodynamic characteristics, as measured by the C_L to C_D ratio, can be readily obtained at higher C_L, see figure 15.

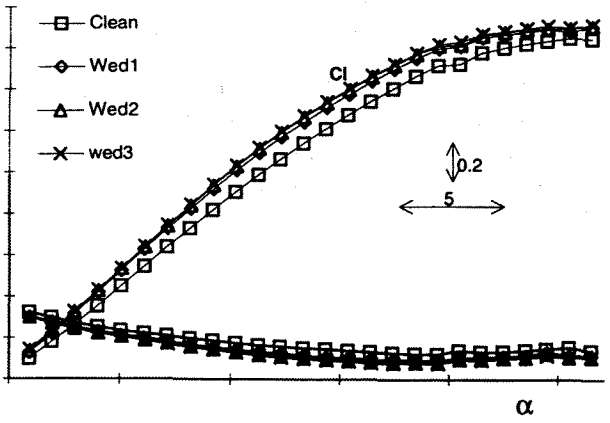

Figure 13. Lift and moment coefficients of the wing body configuration.

The need for a design tool

It is an evident that trailing edge thickness becoming an additional parameter in airfoil design, see figures 1, 5, and 6. In the direct problems, when the airfoil geometry is given, the trailing edge shape must be well taken care.

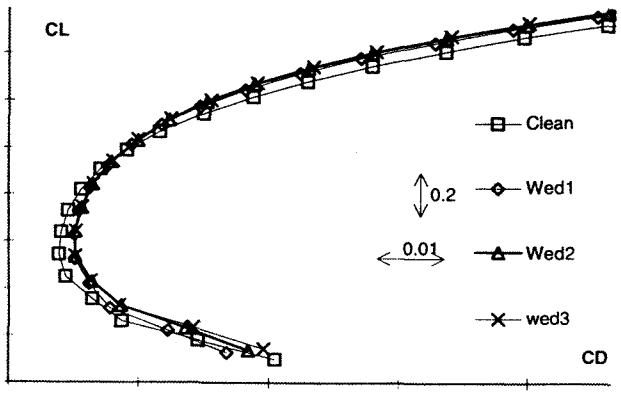

Figure 14. Drag coefficient of the wing body configuration.

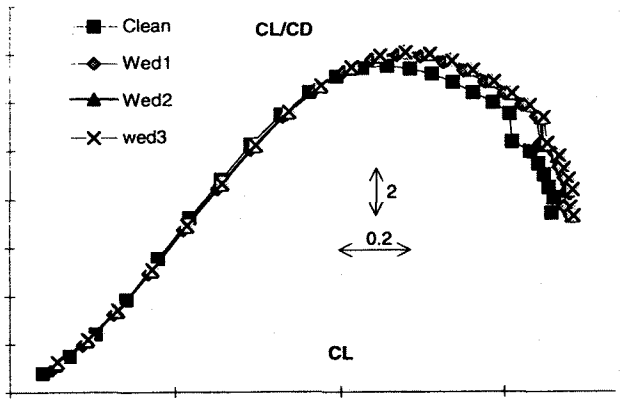

Figure 15. Lift to drag ratio of the wing body configuration.

Methods that deal with closed trailing edge only will certainly not suitable for analysis of airfoil with thick trailing edges. The trailing edge region of an airfoil is too sensitive to the pressure distribution, hence it is very difficult to devise a closing extrapolation. Methods based on field flow analysis are usually capable to deal with airfoils with thick trailing edges, for example the method due to Drela [1]. Panel methods are usually also capable to deal with such airfoils, for example the method due to Sudarmawan [2]. Nevertheless, methods such as [1] and [2] are not suitable for design, by inverse method, to obtain thick trailing edge airfoils. Methods developed with special attention to the thick trailing edges are for example those due to Bauer [3] and Volpe [4]. However, as known to the author, those methods do not have direct control to the trailing edge thickness as admitted by the author [4].

The present author has proposed a method based on conformal mapping, for direct and inverse problems having a full control to the trailing edge thickness [5]. The method utilize the following Laurent series.

$$\frac{dz}{d\varsigma} = 1 + \frac{B}{\varsigma} + \frac{C_1}{\varsigma^2} + \frac{C_2}{\varsigma^3} + \ldots \qquad (5)$$

where the flow field in the airfoil plane (z-plane) is related to the flow field exterior to a circle in the ς-plane. In the direct problem, dz are known, the corresponding $d\varsigma$ and the series coefficients are to be solved for. The coefficient B is related to the trailing edge gap by

$$B = Z_{TE} / 2\pi i \qquad (6)$$

Where Z_{TE} is the vector pointing from the upper trailing edge corner to the lower trailing edge corner. The coefficients C_n are determined by

using residue analysis. In an inverse problem, the left hand side of (5) is written in the form

$$\frac{dz}{d\varsigma} = \frac{U_c}{U_a} e^{i(\omega-\theta+\pi/2)} \qquad (7)$$

Where U_a is specified, U_c is determined from the compatibility conditions between the surface flows in the z- and ς-planes, θ is the polar coordinate of the corresponding point ς on the circle, and ω is the angle of the airfoil surface tangent. In this inverse case, hence, U_c/U_a, and ς are known, the ω and C_n are to be solved for. The coefficient B are determined from the trailing edge gap specification. Thus, the trailing edge gap is a quantity to be prescribed in addition to the pressure distribution. The compatibility condition between the surface flows in the z- and ς-planes are explained in [5] can also be found in [6].
Having a full control on the trailing edge gap, one will have a more freedom in specifying pressure distribution in an inverse problem. As an example see figure 16 below where an inverse problem will result in a self intersecting trailing edge airfoil when the trailing edge gap should be zero. Having the trailing edge gap as an additional parameter, a realistic solution can be obtained. Otherwise, one tends to modify the prescribed pressure distribution to avoid geometry of negative thickness, see example given in [6]

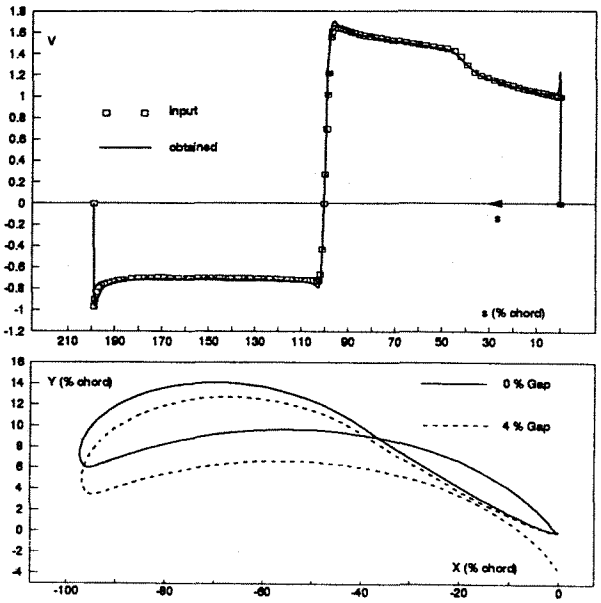

Figure 16. Trailing edge gap as an additional parameter in an inverse problem.

References

1. Giles, M.B. and Drela, M.: Two-dimensional transonic aerodynamic design method. AIAA Journal vol.25 nr.9, September 1987.
2. Sudarmawan, A. and Winarto, H. : Panel method using uniform vortex distribution with Diriclet boundary condition, SITRA proceeding 1991, Bandung, Indonesia.
3. Bauer, F., Garabedian, P., Korn, D., Jameson, A. : Lecture notes in economics and mathematical systems, Supercritical Wing Sections II, Springer-Verlag, 1975.
4. Volpe, G.: Inverse design of airfoil contours: Constraints, numerical method, and applications, AGARD CP-463, 1989.
5. Sardjadi, D. : Enhanced Conformal Mapping Methods for Airfoil Design and Analysis, (thesis draft), Delft University of Technology, The Netherlands, 1996.
6. Strand, T.: Exact method of designing airfoils with given velocity distribution in incompressible flow, Journal of Aircraft, Vol.10 No.11, November 1973.